The CSP was decreased to 60 mmHg for 4–6 min, and then increased every minute from 60 to 180 mmHg using 20-mmHg increments. At least four step cycles were performed under control conditions while Ringer's solution was continuously administered (6 ml kg^{-1} h^{-1}). After recording the control data, the intravenous Ringer's solution was replaced with that containing ANG II (167 ng kg^{-1} min^{-1}). The dose of ANG II was chosen to induce a significant pressor effect based on previous studies [16, 17]. At least three step cycles were performed during ANG II administration.

Data analysis

Data were sampled at 200 Hz using a 16-bit analog-to-digital converter and stored on the hard disk of a dedicated laboratory computer system. To quantify the open-loop static characteristics of the carotid sinus baroreflex, mean values of SNA, AP and HR were calculated during the last 10 s at each CSP level. The effects of ANG II were assessed during the third step cycle after ANG II administration began, at which point the hemodynamic responses to ANG II appeared to reach steady state. Comparisons were made against two control step cycles (control 1 and control 2, see Fig. 1). In each animal, the SNA noise level recorded after the administration of hexamethonium bromide was set to zero. The SNA values obtained at a CSP level of 60 mmHg during control 1 and control 2 were averaged and defined as 100%.

The open-loop characteristics of the AP, SNA and HR responses as functions of CSP were quantified by fitting a four-parameter logistic function to the obtained data as follows [18]:

$$y = \frac{P_1}{1 + \exp[P_2(\mathrm{CSP} - P_3)]} + P_4.$$

where y represents AP, SNA or HR; P_1 is the response range (the difference between the maximum and minimum values of y); P_2 is a slope coefficient; P_3 is the midpoint in CSP; P_4 is the minimum value of y. The maximum gain or maximum slope of the sigmoidal curve was obtained from $P_1P_2/4$.

The open-loop characteristics of the baroreflex peripheral arc (i.e., SNA–AP relation) were quantified using linear regression analysis as follows:

$$\mathrm{AP} = a \times \mathrm{SNA} + b.$$

where a and b represent the slope and intercept of the regression line, respectively.

Statistical analysis

All parameters were compared among control 1, control 2 and ANG II conditions using repeated-measures analysis of variance [19]. When there was a significant difference among the three conditions, all pairwise comparisons were performed using the Student-Neuman-Keuls test. Differences were considered significant at $P < 0.05$. All data are expressed as mean and SE values.

Results

Typical experimental recordings are shown in Fig. 1. The stepwise input from 60 to 180 mmHg was imposed repeatedly on CSP. An increase in CSP decreased SNA. m-SNA represents the 5-s moving-average signal of the percentage of SNA. AP and HR were also decreased in response to increases in CSP. After ANG II administration was initiated, the levels of SNA, AP and HR all increased compared to the levels before ANG II administration. The responses in SNA, AP and HR to the CSP input appeared to be preserved. Data obtained from the three boxes with dashed lines (control 1, control 2 and ANG II) were used for the statistical analysis.

The open-loop characteristics of the total baroreflex revealed sigmoidal nonlinearity (Fig. 2a). No significant differences were observed between the two control conditions. ANG II significantly increased the minimum AP without affecting the response range, slope coefficient or midpoint in CSP (Table 1). The maximum gain of the total baroreflex was unchanged. The open-loop characteristics of the baroreflex control of HR also approximated sigmoidal nonlinearity (Fig. 2b), and no significant differences were observed between the two control conditions. ANG II significantly increased the minimum HR without affecting the response range, slope coefficient or midpoint in CSP (Table 1). The maximum slope of the baroreflex control of HR was unchanged.

The total baroreflex was decomposed into the neural and peripheral arc subsystems. The open-loop characteristics of the baroreflex neural arc revealed sigmoidal nonlinearity (Fig. 3a). There were no significant differences between the two control conditions. ANG II significantly increased the minimum SNA (Table 1). Although the midpoint in CSP was lower in ANG II than in control 1, the difference was not significant when compared with control 2. ANG II did not affect the response range, slope coefficient or the maximum slope of the baroreflex control of SNA. The open-loop characteristics of the baroreflex peripheral arc approximated a straight line (Fig. 3b). There were no significant differences between the two control conditions. ANG II significantly increased the intercept of the regression line (Table 1). AP at 100% SNA did not change significantly, suggesting that the slope of the regression line could be shallower under the ANG II condition. The slope of the

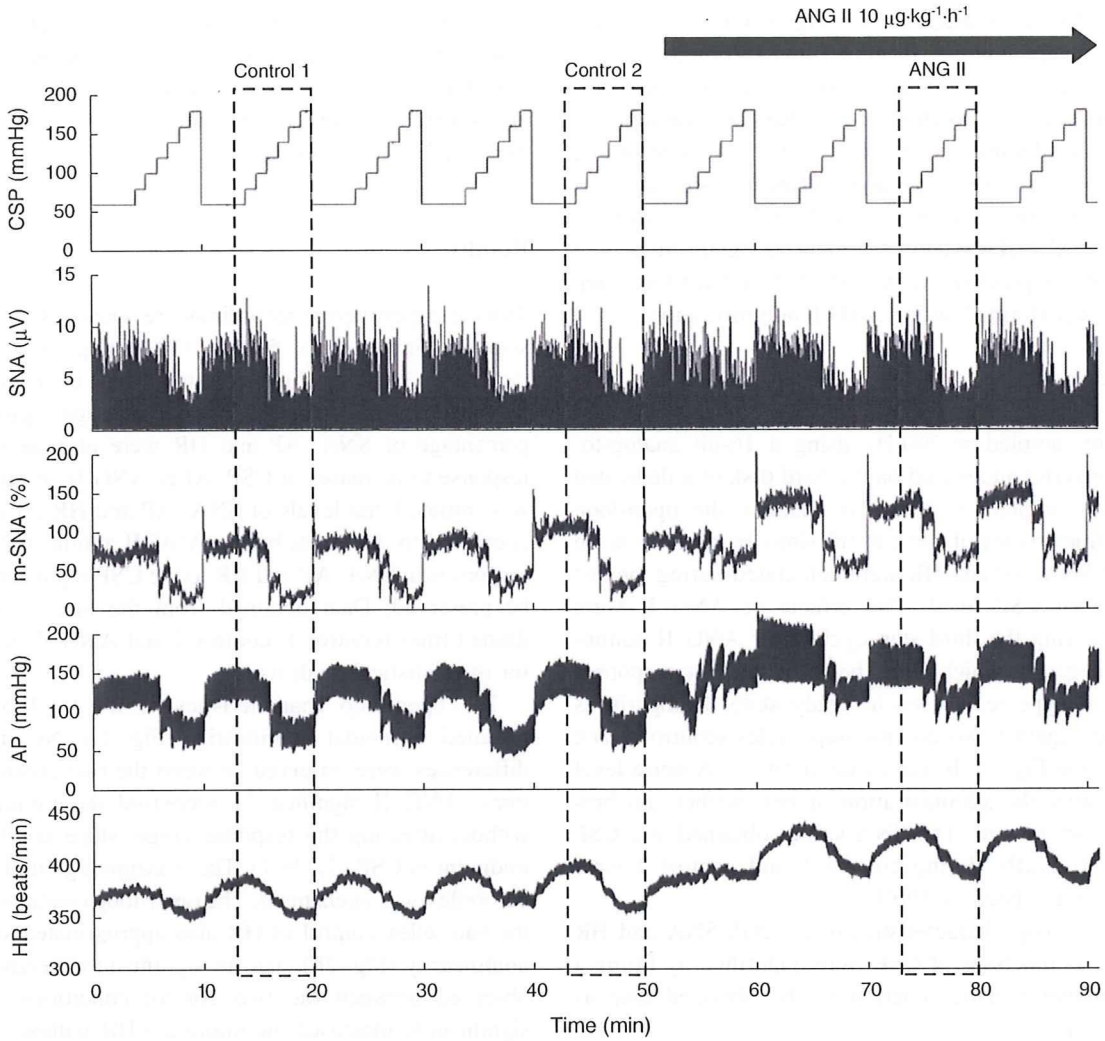

Fig. 1 Typical recordings of carotid sinus pressure (*CSP*), splanchnic sympathetic nerve activity (*SNA*), the 5-s moving-average signal of the percentage of SNA (*m-SNA*), systemic arterial pressure (*AP*) and heart rate (*HR*). CSP was changed stepwise from 60 to 180 mmHg in 20-mmHg increments every minute. Angiotensin II (ANG II) was administered intravenously while the CSP perturbation was continued. ANG II significantly increased SNA, AP and HR. Reflex responses in SNA, AP and HR were not attenuated in the presence of ANG II. *Dashed boxes* indicate the step cycles used for the statistical analysis

regression line, however, was not statistically different among the three conditions.

An equilibrium diagram or a balance diagram was obtained by drawing the neural and peripheral arcs using SNA as the common abscissa and CSP or AP as an ordinate [20–22]. Figure 4 illustrates the equilibrium diagrams under the control 2 (dashed line) and ANG II (solid line) conditions, which were drawn based on the mean parameter values from the logistic function and regression line. Open and filled circles represent the closed-loop operating points under the control 2 and ANG II conditions, respectively. Although AP at the closed-loop operating point was significantly increased by the intravenous ANG II, SNA at the closed-loop operating point was unchanged (Table 1). If ANG II affected the peripheral arc alone, the closed-operating point may have been located at the point depicted by the open triangle. If ANG II affected the neural arc alone, the closed-loop operating point may have been located at the point depicted by the filled triangle.

Discussion

Effects of ANG II on open-loop baroreflex control of SNA

Intravenous ANG II at 167 ng kg^{-1} min^{-1} shifted the open-loop baroreflex control of splanchnic SNA toward higher SNA values without attenuating the size of the response range (Fig. 3a; Table 1). The maximum slope was

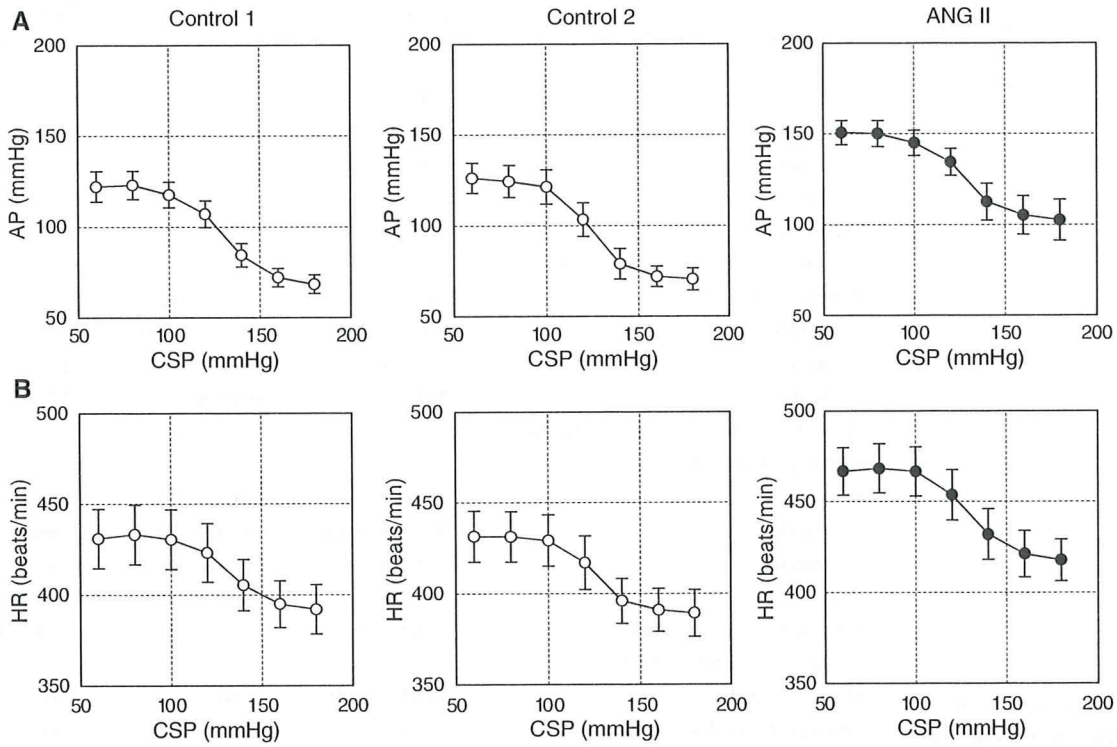

Fig. 2 **a** Averaged input–output relation of the total baroreflex. AP decreased in response to an increase in the CSP. ANG II increased AP, while the range of the AP response was preserved. **b** Averaged input–output relation of the arterial baroreflex control of HR. HR decreased in response to an increase in the CSP. ANG II increased the HR, while the range of the HR response was preserved

unaltered, which agreed with a previous study from our laboratory in which intravenous ANG II at 100 ng kg^{-1} min^{-1} did not change the dynamic gain of the neural arc in anesthetized rabbits [23]. In contrast, Sanderford and Bishop demonstrated that ANG II at 10 or 20 ng kg^{-1} min^{-1} significantly reduced the maximum renal SNA and attenuated the range of baroreflex control of renal SNA in conscious rabbits [9, 24]. On the other hand, Tan et al. [12] demonstrated that intravenous ANG II at 400 ng kg^{-1} min^{-1} did not increase the levels of renal SNA in anesthetized rats. The regional differences in SNA may partly explain the conflicting results, because Fukiyama [25] noted that ANG II infusion (3.5–9.5 ng kg^{-1} min^{-1}) through the vertebral artery resulted in an increase in splanchnic SNA, a transient increase followed by a decrease in renal SNA, and no change in cardiac SNA in anesthetized dogs.

Activation of the renin–angiotensin system contributes to the pathologic sympathoexcitation observed in such cardiovascular diseases as chronic heart failure. In addition to the augmented cardiac sympathetic reflex, impairment of the arterial baroreflex is thought to contribute to sympathoexcitation [13]. The present results indicate that ANG II may increase SNA, but it does not attenuate baroreflex control of SNA such that the magnitude of the SNA response to the input pressure change is preserved (Fig. 3a). ANG II also did not attenuate the gain of the total baroreflex estimated by the magnitude of the AP response to the input pressure change (Fig. 2a). Therefore, the observed weakening of the baroreflex reported in patients with chronic heart failure may not be readily explainable by an acute effect of high circulating levels of ANG II.

Several studies have demonstrated that ANG II-induced hypertension does not decrease SNA via the arterial baroreflex compared to equivalent hypertension induced by phenylephrine [10, 12, 26]. Although those results seem to be consistent with the idea that ANG II blunts the arterial baroreflex, the experimental protocol is confusing, and the interpretation could be wrong as follows. The intersection between the neural and peripheral arcs in the baroreflex equilibrium diagram conforms to the closed-loop operating point [21, 27, 28]. In the present study, ANG II significantly increased AP without significant changes in SNA at the closed-loop operating point (Fig. 4, open vs. filled circles; Table 1). If we calculate the baroreflex control of SNA based on ANG II-induced hypertension, therefore, we would incorrectly conclude that the baroreflex does not control SNA. If we observe the SNA response to changes in

Table 1 Effects of intravenous angiotensin II (ANG II) on the parameters of logistic functions and regression lines of the open-loop baroreflex characteristics

	Control 1	Control 2	ANG II
Total baroreflex, CSP–AP relation			
P_1 (mmHg)	56.2 ± 7.2	56.3 ± 6.4	49.7 ± 6.2
P_2 ($mmHg^{-1}$)	0.116 ± 0.019	0.118 ± 0.015	0.094 ± 0.013
P_3 (mmHg)	129.2 ± 3.5	124.5 ± 2.8	125.7 ± 3.2
P_4 (mmHg)	67.6 ± 4.6	69.7 ± 5.8	101.4 ± 10.9**,††
Maximum gain	1.57 ± 0.28	1.58 ± 0.22	1.20 ± 0.25
Baroreflex control of HR, CSP–HR relation			
P_1(beats/min)	41.7 ± 5.1	43.9 ± 6.2	51.2 ± 3.8
P_2 ($mmHg^{-1}$)	0.123 ± 0.027	0.133 ± 0.018	0.099 ± 0.013
P_3 (mmHg)	131.8 ± 3.8	125.8 ± 3.6	129.1 ± 2.6
P_4 (beats/min)	391.1 ± 13.7	388.0 ± 12.6	417.4 ± 11.5**,††
Maximum slope (beats min^{-1} $mmHg^{-1}$)	1.11 ± 0.12	1.39 ± 0.23	1.28 ± 0.19
Neural arc, CSP–SNA relation			
P_1 (%)	69.6 ± 5.7	66.5 ± 7.4	78.9 ± 9.1
P_2 ($mmHg^{-1}$)	0.110 ± 0.016	0.124 ± 0.015	0.098 ± 0.011
P_3 (mmHg)	133.2 ± 3.8	127.3 ± 3.1	126.0 ± 3.4*
P_4 (%)	33.3 ± 5.4	35.0 ± 6.4	56.5 ± 11.5*,†
Maximum slope (%/mmHg)	1.94 ± 0.34	2.02 ± 0.33	2.04 ± 0.42
Peripheral arc, SNA–AP relation			
Slope, a (mmHg/%)	0.85 ± 0.09	0.86 ± 0.06	0.66 ± 0.10
Intercept, b (mmHg)	37.8 ± 5.2	36.9 ± 5.5	68.0 ± 10.6**,††
AP at 100% SNA (mmHg)	122.7 ± 9.9	122.7 ± 7.0	134.4 ± 4.9
Operating point			
AP (mmHg)	111.4 ± 5.0	110.3 ± 5.1	128.1 ± 4.4**,††
SNA (%)	90.6 ± 7.4	85.8 ± 2.1	94.3 ± 5.9

Data are mean and SE values

CSP Carotid sinus pressure, *AP* arterial pressure, *HR* heart rate, *SNA* sympathetic nerve activity

* $P < 0.05$ and ** $P < 0.01$ from control 1, † $P < 0.05$ and †† $P < 0.01$ from control 2

CSP, however, the baroreflex should be able to control SNA in the presence of ANG II (Fig. 3a). Lumbers et al. [29] pointed out a problem regarding the use of ANG II-induced hypertension as an input perturbation to evaluate the baroreflex.

Effects of ANG II on the baroreflex peripheral arc

The open-loop system characteristics of the baroreflex peripheral arc, assessed using the AP response as a function of SNA, approximated a straight line under both control and ANG II-treated conditions (Fig. 3b), suggesting that the splanchnic SNA may represent changes in systemic SNA that controlled the AP. ANG II significantly increased the intercept of the regression line, reflecting its direct vasoconstrictive effect (Table 1). Because the AP at 100% SNA did not differ among the three conditions, the slope could be shallower in the presence of ANG II. In other words, ANG II appears to elevate the AP to a greater extent for the lower SNA range. Although both the modulation of sympathetic neurotransmission and direct vasoconstriction contribute to the elevation of AP, the fact that ANG II enhances the sympathetic neurotransmission more with a lower stimulation frequency [30, 31] may, in part, account for the greater ANG II-induced increase in AP for the lower SNA range.

Effects of ANG II on the open-loop sympathetic baroreflex control of HR

The baroreflex control of HR showed changes similar to those observed for SNA. Intravenous ANG II increased both the minimum and maximum HR while not significantly affecting the response range of HR or the maximum slope of the response (Fig. 2b; Table 1). The midpoint in CSP was not changed by ANG II. Therefore, the open-loop baroreflex control of HR shifted upward to higher HR values without a concomitant rightward shift to higher CSP values in the present study. In contrast, previous studies reported a rightward shift in the baroreflex control of HR toward higher input pressure values during acute [11, 32] and chronic [33] administration of ANG II in conscious rabbits. Reid and Chou [32] indicated that the inhibition of vagal tone to the heart played a significant role in resetting the baroreflex control of HR in conscious rabbits. It is likely that the rightward shift in the baroreflex control of

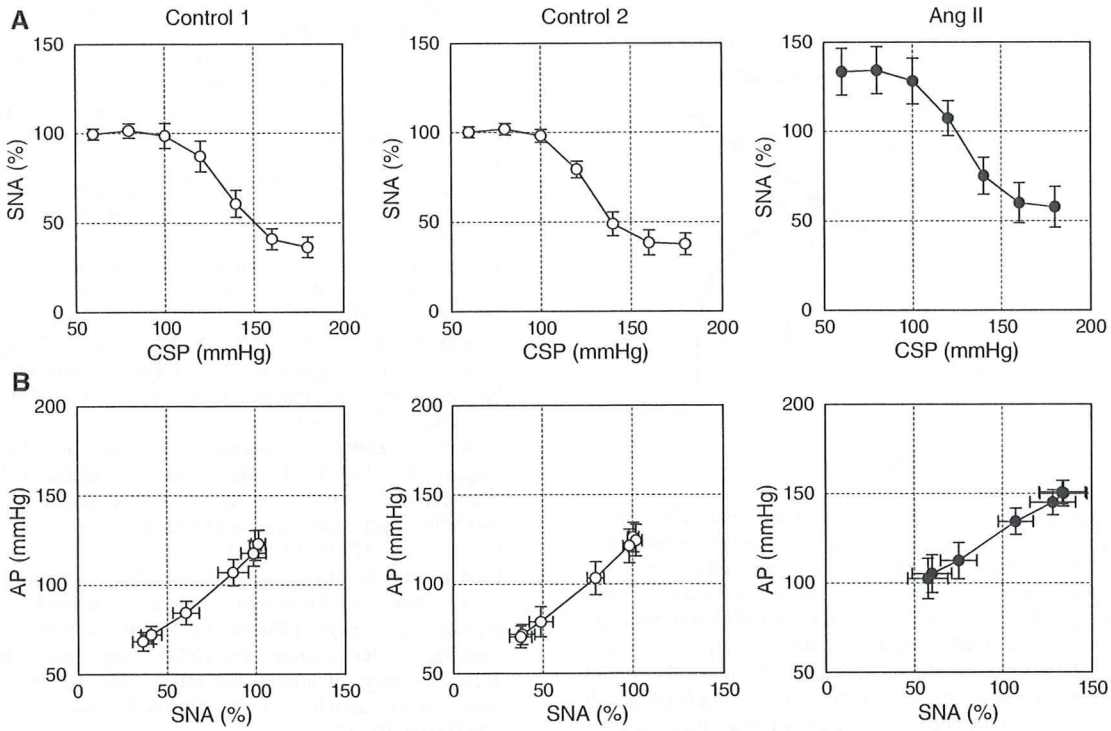

Fig. 3 **a** Averaged input–output relation of the baroreflex neural arc or the arterial baroreflex control of SNA. SNA decreased in response to an increase in the CSP. ANG II increased SNA, while the range of the SNA response was preserved. **b** Averaged input–output relation of the baroreflex peripheral arc. AP increased in response to an increase in SNA. ANG II increased the AP, an effect that was greater for lower SNA

HR by ANG II was not observed in the present study because the vagal nerves were sectioned.

Limitations

First, we performed the experiments in anesthetized animals, and comparisons with results obtained in conscious animals should be made carefully. Circulating levels of ANG II may vary under anesthesia, which could have affected the present results. For instance, reported plasma ANG II concentration in pithed rats is approximately 400 pg/ml [16], which exceeds the plasma ANG II concentration reported in rats with heart failure [34]. Second, although the dose of ANG II used in the present study was within or below those used in previous studies in rats [12, 16, 17], Brown et al. demonstrated that intravenous ANG II at 20 and 270 ng kg^{-1} min^{-1} increased the plasma ANG II concentration from approximately 80 pg/ml to 140 and 2,000 pg/ml, respectively [35]. Based on those data, the plasma ANG II concentration might have been increased beyond a physiologically relevant range to approximately 1,200 pg/ml in the present study. Therefore, the observed effect of ANG II on the arterial baroreflex should be interpreted as pharmacologic. Effects of circulating ANG II can be different when examined in different doses. Third, there was large variation in HR values among the animals (Fig. 2b). Increasing the number of animals would reduce this variation. Nevertheless, data from the eight rats was sufficient to perform statistical analyses and draw reasonable conclusions. Fourth, we occluded the common carotid arteries to isolate the carotid sinuses. Although the vertebral arteries were kept intact and the effects of ANG II were examined using the same preparation, the possibility cannot be ruled out that the carotid occlusion affected the present results. Finally, we cut the vagal nerves to obtain the open-loop condition for the carotid sinus baroreflex. Further studies are needed to clarify the effects of ANG II on the baroreflex control of the cardiovascular system through the vagal system.

Conclusion

The present study indicates that high circulating levels of ANG II significantly increased splanchnic SNA but did not acutely attenuate the range of arterial baroreflex control of SNA. The ranges of the total baroreflex response and the baroreflex control of HR were also preserved during ANG

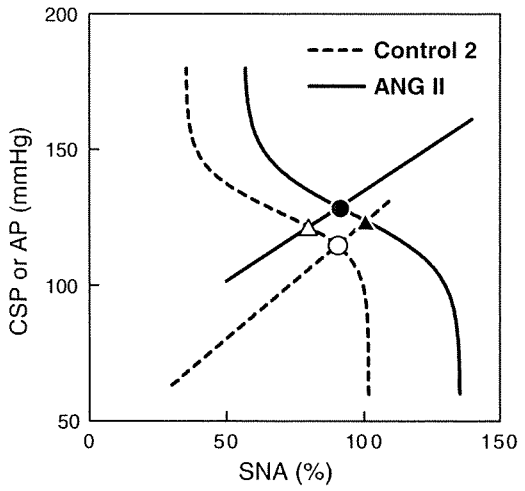

Fig. 4 Equilibrium diagrams between the arterial baroreflex neural and peripheral arcs. The *dashed* and *solid curves* represent the open-loop characteristics of the baroreflex neural arc under the control and ANG II-treated conditions, respectively. The *dashed* and *solid lines* represent the open-loop characteristics of the baroreflex peripheral arc under the control and ANG II-treated conditions, respectively. The *open circle* indicates the closed-loop operating point under the control condition. ANG II causes an upward shift in the peripheral arc. If ANG II does not affect the neural arc, the closed-loop operating point would be at the point depicted by the *open triangle*. In this case, the estimation of baroreflex control of SNA based on the closed-loop operating points (the *open circle* and *open triangle*) approximates the slope of the baroreflex neural arc (*dashed curve*). ANG II, however, causes a rightward shift in the neural arc. Thus, the estimation of the baroreflex control of SNA based on closed-loop operating points (the *open* and *filled circles*) does not match the slope of the neural arc under either the control (*dashed curve*) or ANG II-treated condition (*solid curve*)

II administration. ANG II does modify the arterial baroreflex in that it increases SNA at a given baroreceptor pressure level but does not appear to attenuate the range of arterial baroreflex control of SNA, HR or AP.

Acknowledgments This study was supported by Health and Labour Sciences Research Grants (H18-nano-Ippan-003, H19-nano-Ippan-009, H20-katsudo-Shitei-007, and H21-nano-Ippan-005) from the Ministry of Health, Labour and Welfare of Japan; by a Grant-in-Aid for Scientific Research (No. 20390462) from the Ministry of Education, Culture, Sports, Science and Technology of Japan; and by the Industrial Technology Research Grant Program from the New Energy and Industrial Technology Development Organization (NEDO) of Japan.

References

1. Ikeda Y, Kawada T, Sugimachi M, Kawaguchi O, Shishido T, Sato T, Miyano H, Matsuura W, Alexander J Jr, Sunagawa K (1996) Neural arc of baroreflex optimizes dynamic pressure regulation in achieving both stability and quickness. Am J Physiol 271:H882–H890
2. Kawada T, Yamamoto K, Kamiya A, Ariumi H, Michikami D, Shishido T, Sunagawa K, Sugimachi M (2005) Dynamic characteristics of carotid sinus pressure-nerve activity transduction in rabbits. Jpn J Physiol 55:157–163
3. Sato T, Kawada T, Shishido T, Miyano H, Inagaki M, Miyashita H, Sugimachi M, Kneupfer MM, Sunagawa K (1998) Dynamic transduction properties of in situ baroreceptors of rabbit aortic depressor nerve. Am J Physiol Heart Circ Physiol 274:H358–H365
4. Chapleau MW, Abboud FM (1987) Contrasting effects of static and pulsatile pressure on carotid baroreceptor activity in dogs. Circ Res 61:648–658
5. Kawada T, Fujiki N, Hosomi H (1992) Systems analysis of the carotid sinus baroreflex system using a sum-of-sinusoidal input. Jpn J Physiol 42:15–34
6. Kawada T, Yanagiya Y, Uemura K, Miyamoto T, Zheng C, Li M, Sugimachi M, Sunagawa K (2002) Input-size dependence of the baroreflex neural arc transfer characteristics. Am J Physiol Heart Circ Physiol 284:H404–H415
7. Kawada T, Zheng C, Yanagiya Y, Uemura K, Miyamoto T, Inagaki M, Shishido T, Sugimachi M, Sunagawa K (2002) High-cut characteristics of the baroreflex neural arc preserve baroreflex gain against pulsatile pressure. Am J Physiol Heart Circ Physiol 282:H1149–H1156
8. Reid IA (1992) Interactions between ANG II, sympathetic nervous system, and baroreceptor reflexes in regulation of blood pressure. Am J Physiol Endocrinol Metab 262:E763–E778
9. Sanderford MG, Bishop VS (2000) Angiotensin II acutely attenuates range of arterial baroreflex control of renal sympathetic nerve activity. Am J Physiol Heart Circ Physiol 279:H1804–H1812
10. McMullan S, Goodchild AK, Pilowsky PM (2007) Circulating angiotensin II attenuates the sympathetic baroreflex by reducing the barosensitivity of medullary cardiovascular neurons in the rat. J Physiol 582:711–722
11. Kumagai K, Reid IA (1994) Angiotensin II exerts differential actions on renal nerve activity and heart rate. Hypertension 24:451–456
12. Tan PS, Killinger S, Horiuchi J, Dampney RA (2007) Baroreceptor reflex modulation by circulating angiotensin II is mediated by AT_1 receptors in the nucleus tractus solitarius. Am J Physiol Regul Integr Comp Physiol 293:R2267–R2278
13. Zucker IH (2006) Novel mechanisms of sympathetic regulation in chronic heart failure. Hypertension 48:1005–1011
14. Shoukas AA, Callahan CA, Lash JM, Haase EB (1991) New technique to completely isolate carotid sinus baroreceptor regions in rats. Am J Physiol Heart Circ Physiol 260:H300–H303
15. Sato T, Kawada T, Miyano H, Shishido T, Inagaki M, Yoshimura R, Tatewaki T, Sugimachi M, Alexander J Jr, Sunagawa K (1999) New simple methods for isolating baroreceptor regions of carotid sinus and aortic depressor nerves in rats. Am J Physiol Heart Circ Physiol 276:H326–H332
16. Grant TL, McGrath JC (1988) Interactions between angiotensin II, sympathetic nerve-mediated pressor response and cyclo-oxygenase products in the pithed rat. Br J Pharmacol 95:1220–1228
17. Haywood JR, Fink GD, Buggy J, Phillips MI, Brody MJ (1980) The area postrema plays no role in the pressor action of angiotensin in the rat. Am J Physiol Heart Circ Physiol 239:H108–H113
18. Kent BB, Drane JW, Blumenstein B, Manning JW (1972) A mathematical model to assess changes in the baroreceptor reflex. Cardiology 57:295–310
19. Glantz SA (2002) Primer of biostatistics, 5th edn. McGraw-Hill, New York
20. Mohrman DE, Heller LJ (2006) Cardiovascular physiology, 6th edn. McGraw Hill, New York, pp 172–177
21. Sato T, Kawada T, Inagaki M, Shishido T, Takaki H, Sugimachi M, Sunagawa K (1999) New analytic framework for

understanding sympathetic baroreflex control of arterial pressure. Am J Physiol Heart Circ Physiol 276:H2251–H2261
22. Kawada T, Shishido T, Inagaki M, Zheng C, Yanagiya Y, Uemura K, Sugimachi M, Sunagawa K (2002) Estimation of baroreflex gain using a baroreflex equilibrium diagram. Jpn J Physiol 52:21–29
23. Kashihara K, Takahashi Y, Chatani K, Kawada T, Zheng C, Li M, Sugimachi M, Sunagawa K (2003) Intravenous angiotensin II does not affect dynamic baroreflex characteristics of the neural or peripheral arc. Jpn J Physiol 53:135–143
24. Sanderford MG, Bishop VS (2002) Central mechanisms of acute ANG II modulation of arterial baroreflex control of renal sympathetic nerve activity. Am J Physiol Heart Circ Physiol 282:H1592–H1602
25. Fukiyama K (1972) Central action of angiotensin and hypertension—increased central vasomotor outflow by angiotensin. Jpn Circ J 36:599–602
26. Guo GB, Abboud FM (1984) Angiotensin II attenuates baroreflex control of heart rate and sympathetic activity. Am J Physiol Heart Circ Physiol 246:H80–H89
27. Kamiya A, Kawada T, Yamamoto K, Michikami D, Ariumi H, Uemura K, Zheng C, Shimizu S, Aiba T, Miyamoto T, Sugimachi M, Sunagawa K (2005) Resetting of the arterial baroreflex increases orthostatic sympathetic activation and prevents postural hypotension in rabbits. J Physiol 566:237–246
28. Yamamoto K, Kawada T, Kamiya A, Takaki H, Miyamoto T, Sugimachi M, Sunagawa K (2004) Muscle mechanoreflex induces the pressor response by resetting the arterial baroreflex neural arc. Am J Physiol Heart Circ Physiol 286:H1382–H1388
29. Lumbers ER, McCloskey DI, Potter EK (1979) Inhibition by angiotensin II of baroreceptor-evoked activity in cardiac vagal efferent nerves in the dog. J Physiol 294:69–80
30. Hughes J, Roth RH (1971) Evidence that angiotensin enhances transmitter release during sympathetic nerve stimulation. Br J Phrmacol 41:239–255
31. Zimmerman BG, Gomer SK, Liao JC (1972) Action of angiotensin on vascular adrenergic nerve endings: facilitation of norepinephrine release. Federation Proc 31:1344–1350
32. Reid IA, Chou L (1990) Analysis of the action of angiotensin II on the baroreflex control of heart rate in conscious rabbits. Endocrinology 126:2749–2756
33. Brooks VL (1995) Chronic infusion of angiotensin II resets baroreflex control of heart rate by an arterial pressure-independent mechanism. Hypertension 26:420–424
34. Schunkert H, Tang SS, Litwin SE, Diamant D, Riegger G, Dzau VJ, Ingelfinger JR (1993) Regulation of intrarenal and circulating renin–angiotensin systems in severe heart failure in the rat. Cardiovasc Res 27:731–735
35. Brown AJ, Casals-Stenzel J, Gofford S, Lever AF, Morton JJ (1981) Comparison of fast and slow pressor effects of angiotensin II in the conscious rat. Am J Physiol Heart Circ Physiol 241:H381–H388

Life Sciences 85 (2009) 597–601

Contents lists available at ScienceDirect

Life Sciences

journal homepage: www.elsevier.com/locate/lifescie

Detection of endogenous acetylcholine release during brief ischemia in the rabbit ventricle: A possible trigger for ischemic preconditioning

Toru Kawada [a,*], Tsuyoshi Akiyama [b], Shuji Shimizu [a], Atsunori Kamiya [a], Kazunori Uemura [a], Meihua Li [a], Mikiyasu Shirai [b], Masaru Sugimachi [a]

[a] Department of Cardiovascular Dynamics, Advanced Medical Engineering Center, National Cardiovascular Center Research Institute, Japan
[b] Department of Cardiac Physiology, National Cardiovascular Center Research Institute, Japan

ARTICLE INFO

Article history:
Received 1 July 2009
Accepted 25 August 2009

Keywords:
Acetylcholine
Cardiac microdialysis
Vagal stimulation
Coronary artery occlusion
Rabbits

ABSTRACT

Aims: To examine endogenous acetylcholine (ACh) release in the rabbit left ventricle during acute ischemia, ischemic preconditioning and electrical vagal stimulation.

Main methods: We measured myocardial interstitial ACh levels in the rabbit left ventricle using a cardiac microdialysis technique. In Protocol 1 ($n=6$), the left circumflex coronary artery (LCX) was occluded for 30 min and reperfused for 30 min. In Protocol 2 ($n=5$), the LCX was temporarily occluded for 5 min. Ten minutes later, the LCX was occluded for 30 min and reperfused for 30 min. In Protocol 3 ($n=5$), bilateral efferent vagal nerves were stimulated at 20 Hz and 40 Hz (10 V, 1-ms pulse duration).

Key findings: In Protocol 1, a 30-min coronary occlusion increased the ACh level from 0.39 ± 0.15 to 7.0 ± 2.2 nM (mean ± SE, $P<0.01$). In Protocol 2, a 5-min coronary occlusion increased the ACh level from 0.33 ± 0.07 to 0.75 ± 0.11 nM ($P<0.05$). The ACh level returned to 0.48 ± 0.10 nM during the interval. After that, a 30-min coronary occlusion increased the ACh level to 2.4 ± 0.49 nM ($P<0.01$). In Protocol 3, vagal stimulation at 20 Hz and 40 Hz increased the ACh level from 0.29 ± 0.06 to 1.23 ± 0.48 ($P<0.05$) and 2.44 ± 1.13 nM ($P<0.01$), respectively.

Significance: Acute ischemia significantly increased the ACh levels in the rabbit left ventricle, which appeared to exceed the vagal stimulation-induced ACh release. Brief ischemia as short as 5 min can also increase the ACh level, suggesting that endogenous ACh release can be a trigger for ischemic preconditioning.

Introduction

Although ventricular vagal innervation is sparser than that observed in the atrium, we have previously demonstrated that electrical vagal stimulation and acute myocardial ischemia significantly increased myocardial interstitial acetylcholine (ACh) levels in the feline left ventricle (Kawada et al. 2000, 2001, 2006a,b, 2007). Potential differences between species, however, suggest that data obtained from the feline left ventricle may not be directly extrapolated to ventricular vagal innervation in other species (Brown 1976; Kilbinger and Löffelholz 1976). Compared with the feline heart, the rabbit heart is more frequently analyzed in investigations of myocardial ischemia and ischemic preconditioning. For instance, Qin et al. (2003) used isolated rabbit hearts to demonstrate that ACh and adenosine induce ischemic preconditioning mimetic effects through different signaling pathways. In our previous study, vagal stimulation increased the level of tissue inhibitor of metalloproteinase-1 (TIMP-1) and reduced the level of endogenous active matrix metalloproteinase-9 (MMP-9) during ischemia–reperfusion injury in the rabbit left ventricle (Uemura et al. 2007). Despite its potential cardioprotective effects against myocardial ischemia, the profile of endogenous ACh release in the rabbit left ventricle is poorly understood *in vivo* owing to the difficulty in detecting low levels of myocardial interstitial ACh. Quantification of endogenous ACh release during myocardial ischemia and electrical vagal stimulation would help understand the potential cardioprotective effects of vagal stimulation. In the present study, we examined the effects of acute myocardial ischemia, ischemic preconditioning, and electrical vagal stimulation on myocardial interstitial ACh levels in the rabbit left ventricle *in vivo* using an improved high-performance liquid chromatography (HPLC) system that allowed us to detect low concentrations of ACh (Shimizu et al. 2009).

Materials and methods

Surgical preparation and protocols

Animal care was conducted in accordance with the *Guiding Principles for the Care and Use of Animals in the Field of Physiological Sciences*, which has been approved by the Physiological Society of

* Corresponding author. Department of Cardiovascular Dynamics, Advanced Medical Engineering Center, National Cardiovascular Center Research Institute, 5-7-1 Fujishirodai, Suita, Osaka 565-8565, Japan. Tel.: +81 6 6833 5012x2427; fax: +81 6 6835 5403.
E-mail address: torukawa@res.ncvc.go.jp (T. Kawada).

0024-3205/$ – see front matter © 2009 Published by Elsevier Inc.
doi:10.1016/j.lfs.2009.08.015

Japan. Japanese white rabbits weighing 2.5 kg to 3.1 kg (2.8 ± 0.1 kg, mean ± SE) were anesthetized via intravenous administration of pentobarbital sodium (30–35 mg/kg) through a marginal ear vein. The animals were ventilated mechanically with room air mixed with oxygen. The anesthetic condition was maintained using a continuous intravenous infusion of urethane (125 mg kg^{-1} h^{-1}) and α-chloralose (20 mg kg^{-1} h^{-1}) through a catheter inserted in the right femoral vein. Mean arterial pressure (AP) was measured using a catheter inserted in the right femoral artery. Heart rate (HR) was measured from an electrocardiogram obtained using a cardiotachometer. The animal was placed in a lateral position, and the left fourth and fifth ribs were partially resected to allow access to the heart. The heart was suspended in a pericardial cradle.

In Protocol 1 ($n = 6$), which was designed to examine the effects of acute myocardial ischemia and reperfusion, a 3-0 silk suture was passed around a branch of the left circumflex coronary artery (LCX); both ends were passed through a polyethylene tube to make a snare to occlude the artery. A dialysis probe was implanted into the anterolateral free wall of the left ventricle perfused by the LCX. After collecting a baseline dialysate sample, the LCX was occluded for 30 min and reperfused for 30 min. After the ischemia–reperfusion protocol was finished, the LCX was occluded again and a 5-ml bolus of 1% methylene blue was injected intravenously to confirm that the dialysis probe had been implanted within the area at risk for myocardial ischemia.

In Protocol 2 ($n = 5$), which was designed to examine the effects of ischemic preconditioning (*i.e.*, a brief ischemic event preceding a major ischemic event), a 3-0 silk suture was passed around a branch of the LCX and both ends were passed through a polyethylene tube to make a snare. Two dialysis probes were implanted into the anterolateral free wall of the left ventricle perfused by the LCX; the probes were separated by at least 5 mm. Combining the dialysate samples obtained from the two dialysis probes increased the time resolution of the ACh measurement. After collecting a baseline dialysate sample, the LCX was temporarily occluded for 5 min which was followed by a 10-min interval. The LCX was then occluded for 30 min and reperfused for 30 min. After the ischemia–reperfusion protocol was completed, the LCX was occluded again and a 5-ml bolus of 1% methylene blue was injected intravenously to confirm that the two dialysis probes had been implanted within the area at risk for myocardial ischemia.

In Protocol 3 ($n = 5$), which was designed to examine the effects of electrical vagal stimulation, the vagus nerves were exposed and sectioned at the neck. Each sectioned vagus nerve was placed on a pair of bipolar platinum electrodes to stimulate the efferent vagus nerve. The nerve and the electrodes were fixed using silicone glue (Kwik-Sil, World Precision Instruments, Sarasota, FL, USA). Two dialysis probes were implanted into the anterolateral free wall of the left ventricle; the probes were separated by at least 5 mm. Dialysate samples obtained from the two dialysis probes were analyzed separately. After collecting baseline dialysate samples, the vagus nerves were stimulated at 20 Hz for 15 min and 40 Hz for 15 min. The stimulation amplitude was 10 V and the pulse duration was 1 ms. The 40-Hz stimulation often caused an initial cardiac arrest for a few seconds and was considered to be the most intensive stimulation in the present experimental settings. The 20-Hz stimulation was arbitrarily selected at a half of the maximum stimulation rate to observe the dependence of the ACh release on the stimulation rate.

At the end of each protocol, the experimental animals were sacrificed with an overdose of intravenous pentobarbital sodium. We performed a postmortem examination and confirmed that the dialysis probe(s) had been implanted within the left ventricular myocardium.

Dialysis technique

We measured dialysate concentrations of ACh as indices of myocardial interstitial ACh levels. The materials and properties of the dialysis probe have been described previously (Akiyama et al. 1994). Briefly, we designed a transverse dialysis probe. A dialysis fiber (length, 8 mm; outer diameter, 310 μm; inner diameter, 200 μm; PAN-1200, 50,000-Da molecular-weight cutoff, Asahi Chemical, Japan) was glued at both ends to polyethylene tubes (length, 25 cm; outer diameter, 500 μm; inner diameter, 200 μm). The dialysis probe was perfused at a rate of 2 μl/min with Ringer's solution containing a cholinesterase inhibitor eserine (100 μM). Dialysate sampling was started from 2 h after probe implantation. In Protocols 1 and 3, one sampling period was set at 15 min, which yielded a sample volume of 30 μl. The actual dialysate sampling lagged behind a given collection period by 5 min owing to the dead space volume between the dialysis membrane and collecting tube. In Protocol 2, one sampling period was set at 5 min to increase the time resolution during the ischemic preconditioning, and dialysate samples from the two dialysis probes were combined to yield a sample volume of 20 μl. The sampling period was changed to 10 min during the main ischemic event to reduce the total number of samples. The amount of ACh in the dialysate was measured using an HPLC system with electrochemical detection (Eicom, Japan) adjusted to measure low levels of ACh (Shimizu et al. 2009). The concentration of ACh was calculated taking the sample volume in account.

Statistical analysis

All data are presented as the mean and SE values. We performed repeated-measures analysis of variance, followed by a Tukey test for all pairwise, multiple comparisons to examine changes in the ACh levels (Glantz 2002). Because the variance of measured ACh levels increased with their mean, statistical analysis was performed after logarithmic conversion of the ACh data (Snedecor and Cochran 1989). The AP and HR data were examined using repeated-measures analysis of variance, followed by a Dunnett's test for multiple comparisons against a single control (Glantz 2002). In Protocols 1 and 3, the baseline value was treated as the single control. In Protocol 2, the value measured just before the main ischemic event was treated as the single control. In all of the statistical analyses, differences were considered significant when $P < 0.05$.

Results

In Protocol 1, the myocardial interstitial ACh levels significantly increased during ischemia compared with the baseline value (Fig. 1). Although the ACh levels declined during reperfusion, they were still significantly higher than the baseline value. Changes in AP and HR are summarized in Table 1. Although AP did not change significantly during ischemia, it decreased significantly throughout the reperfusion period. The HR increased significantly after 30 min of ischemia, and remained high during the reperfusion period with the exception of the last data point.

In Protocol 2, the LCX was occluded for 5 min (ischemic preconditioning) and released for 10 min before the major ischemic event. The brief 5-min occlusion significantly increased the myocardial interstitial ACh level compared with the baseline value (Fig. 2). The ACh levels during the interval between the brief occlusion and the major occlusion did not differ from the baseline value. The ACh levels increased significantly during the major ischemic event compared with the baseline value. Although the ACh levels declined during reperfusion, they were still significantly higher than the baseline value. Changes in AP and HR are summarized in Table 2. Neither AP nor HR changed significantly compared with the respective control values measured after the 10-min middle interval.

In Protocol 3, electrical vagal stimulation significantly increased the myocardial interstitial ACh levels (Fig. 3). The ACh levels returned close to the baseline value just after vagal stimulation was terminated. The AP and HR values were significantly reduced by vagal stimulation (Table 3).

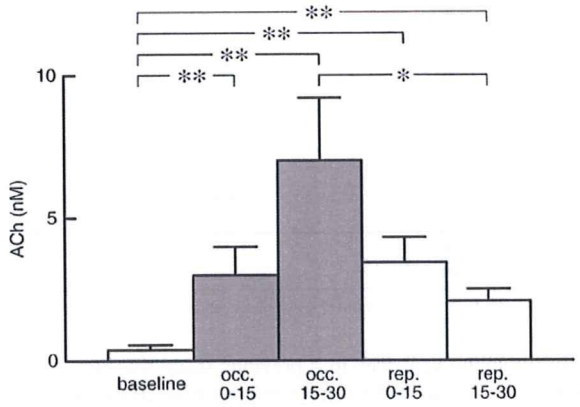

Fig. 1. Changes in the myocardial interstitial ACh levels in Protocol 1. The left circumflex coronary artery was occluded for 30 min and reperfused for 30 min. occ: occlusion; rep: reperfusion. Data are shown as the mean + SE ($n = 6$). $^{*}P < 0.05$ and $^{**}P < 0.01$; Tukey test.

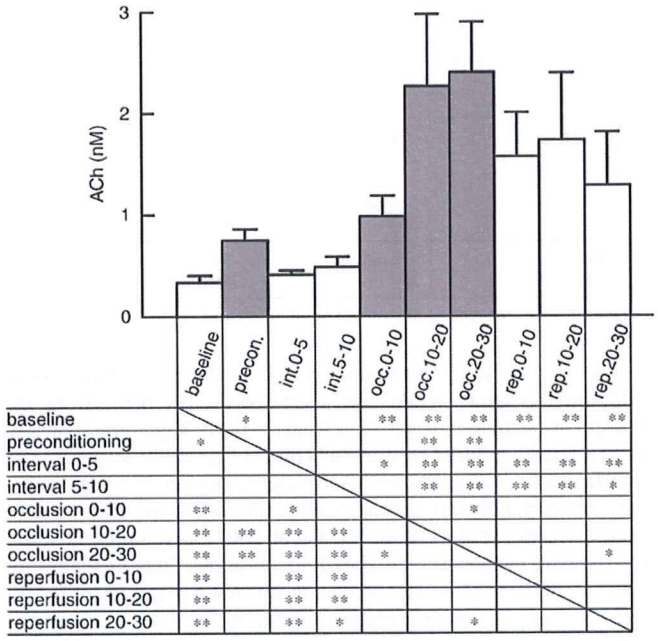

Fig. 2. Changes in the myocardial interstitial ACh levels in Protocol 2. The left circumflex coronary artery was occluded for 5 min. Ten minutes later, the left circumflex coronary artery was occluded for 30 min and reperfused for 30 min. precon: preconditioning; int: interval; occ: occlusion; rep: reperfusion. Data are shown as the mean + SE ($n = 5$). $^{*}P < 0.05$ and $^{**}P < 0.01$; Tukey test.

Discussion

Effects of acute ischemia on myocardial interstitial ACh levels

Acute myocardial ischemia significantly increased myocardial interstitial ACh levels in the ischemic region (Fig. 1). To our knowledge, this is the first report demonstrating ischemia-induced ACh release in the rabbit left ventricle *in vivo*. Because electrical vagal stimulation increased the myocardial interstitial ACh levels (Fig. 3), centrally mediated activation of the efferent vagus nerve could contribute to these effects. LCX occlusion, however, did not decrease the HR significantly (Table 1), suggesting that centrally mediated vagal activation did not have a marked role in the present study. In a previous study, acute myocardial ischemia increased myocardial interstitial ACh levels in vagotomized cats, suggesting an important role of a local release mechanism that is independent of efferent vagal activity (Kawada et al. 2000). Intracellular Ca^{2+} mobilization related to cation-selective stretch-activated channels is thought to be involved in this local release mechanism (Kawada et al. 2000, 2006b). A similar local mechanism may be responsible for ischemia-induced ACh release in the rabbit left ventricle.

In our previous study, topical perfusion of ACh through a dialysis probe increased TIMP-1 levels in the rabbit left ventricle (Uemura et al. 2007). The production of TIMP-1 reduces endogenous levels of active MMP-9, which can limit ventricular remodeling following myocardial ischemia and reperfusion. Whether ischemia-induced ACh release can induce such an anti-remodeling effect remains unanswered, however, because reperfusion reduced the myocardial interstitial ACh levels toward the baseline value. Whether prolonged ischemia for more than 30 min induces sustained elevations of ACh levels is an interesting topic for future studies.

The ACh levels were decreased toward the baseline value upon reperfusion, probably by the washout of ACh from the interstitial fluid. In the case of myocardial interstitial myoglobin levels, the reperfusion further increases the myoglobin levels, suggesting an occurrence of reperfusion injury to the myocardium (Kitagawa et al. 2005). Reoxygenation upon reperfusion rapidly restores the ATP synthesis, which can cause hypercontracture of myofibrils and undesired cytoskeletal lesions (Piper et al. 2004). Because the vagal nerve endings do not have contractile elements, the hypercontracture-induced cell injury does not occur, and the further release of ACh may have been prevented.

Effects of ischemic preconditioning on myocardial interstitial ACh levels

Ischemic preconditioning is a phenomenon in which a brief ischemic event makes the heart resistant to a subsequent ischemic insult (Murry et al. 1986). Acetylcholine, bradykinin, and adenosine are endogenous substances that can induce ischemic preconditioning mimetic effects in the rabbit heart (Liu et al. 1991; Qin et al. 2003; Krieg et al. 2004). In a previous study, we showed that a 5-min ischemic event increased myocardial interstitial ACh levels in the feline ventricle (Kawada et al. 2002). Ischemic preconditioning, however, is not frequently examined in the feline ventricle, making interpretation of these results difficult. In the present study, a 5-min ischemic event caused a significant increase in the ACh level in the rabbit left ventricle (Fig. 2), suggesting that brief ischemia-induced ACh release may serve as a trigger for the ischemic preconditioning. Krieg et al. (2004) demonstrated that ACh triggers preconditioning by sequentially activating Akt and nitric oxide synthase to produce reactive oxygen species. An acetylcholine-induced preconditioning mimetic effect has also been observed in canine (Yao and Gross 1993; Przyklenk and Kloner 1995) and rat (Richard et al. 1995) models.

Table 1
Mean arterial pressure (AP) and heart rate (HR) obtained during Protocol 1 ($n = 6$).

	Baseline	Occlusion 5 min	Occlusion 15 min	Occlusion 30 min	Reperfusion 5 min	Reperfusion 15 min	Reperfusion 30 min
AP(mm Hg)	82 ± 4	77 ± 4	72 ± 5	75 ± 5	72 ± 5*	70 ± 4*	70 ± 2**
HR (beats/min)	247 ± 16	264 ± 14	265 ± 13	280 ± 10**	278 ± 9*	277 ± 8*	274 ± 9

Data are shown as the mean ± SE. $^{*}P < 0.05$ and $^{**}P < 0.01$ vs. baseline using Dunnett's test.

Table 2
Mean arterial pressure (AP) and heart rate (HR) obtained during Protocol 2 ($n=5$).

	Baseline	Preconditioning 5 min	Interval 5 min	Interval 10 min	Occlusion 5 min	Occlusion 10 min
AP(mm Hg)	83±5	77±5	78±4	80±4	78±5	78±5
HR(beats/min)	277±7	282±8	282±7	284±5	285±5	286±6
	Occlusion 20 min	Occlusion 30 min	Reperfusion 5 min	Reperfusion 10 min	Reperfusion 20 min	Reperfusion 30 min
AP(mm Hg)	77±4	78±5	77±5	78±5	77±3	79±3
HR(beats/min)	287±5	289±6	290±5	289±5	290±6	293±5

Data are shown as the mean±SE. No significant differences relative to control values (the value 10 min after the preconditioning) were observed based on Dunnett's test.

In a previous study examining the feline ventricle (Kawada et al. 2002), brief ischemia significantly decreased the HR, highlighting the presence of a significant vagal reflex from the heart. Vagotomy abolished the ACh release induced by brief ischemia in that study, suggesting an important role of centrally mediated vagal activation. The vagal reflex from the heart, however, shows regional differences and varies among species (Thames et al. 1978; Kawada et al. 2007). In the present study, brief ischemia did not decrease the HR significantly (Table 2), suggesting that centrally mediated vagal activation was not a major factor for the brief ischemia-induced ACh release in the rabbit heart.

Rabbits exhibit marked effects from ischemic preconditioning, including reduced infarct size (Cohen et al. 1991; Cason et al. 1997). Although whether the ACh release induced by the brief ischemic event exerted cardioprotective effects was not examined in the present study, there was a notable difference in the changes in AP observed with Protocol 1 and Protocol 2. Although AP decreased significantly upon reperfusion in Protocol 1 (Table 1), it did not change significantly during the major ischemic event in Protocol 2 (Table 2), possibly reflecting preserved cardiac function as a result of the ischemic preconditioning.

Effects of electrical vagal stimulation on myocardial interstitial ACh levels

In the feline left ventricle, electrical vagal stimulation at 20 Hz (10 V, 1-ms pulse duration) increases myocardial interstitial ACh levels to approximately 20 nM as measured with a dialysis fiber 13 mm in length (Kawada et al. 2000). In contrast, electrical vagal stimulation at 20 Hz in the rabbit left ventricle (10 V, 1-ms pulse duration) increased the ACh levels to approximately 1.2 nM as measured with a dialysis fiber 8 mm long (Fig. 3). The small increase in the ACh level detected during electrical vagal stimulation may indicate that vagal innervation is much sparser in the rabbit ventricle

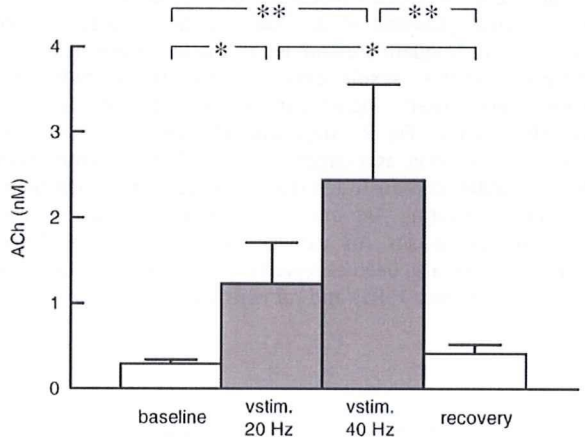

Fig. 3. Changes in the myocardial interstitial ACh levels in Protocol 3. The bilateral efferent vagus nerves were stimulated at 20 Hz for 15 min and 40 Hz for 15 min. Data are shown as the mean + SE ($n=10$, 2 samples from each of the 5 animals). $^{*}P<0.05$ and $^{**}P<0.01$; Tukey test.

than in the feline ventricle. In a previous study that used a dialysis fiber 4 mm in length, right vagal stimulation at 20 Hz increased the dialysate ACh concentration from 0.4±0.2 nM to 0.9±0.3 nM, whereas left vagal stimulation at 20 Hz increased it from 0.3±0.1 nM to 1.0±0.4 nM in the rabbit right ventricle (Shimizu et al. 2009). Considering the bilateral stimulation and fiber length of 8 mm in the present study, the vagal innervation of the left ventricle may be comparable to or slightly sparser than that of the right ventricle.

The dialysis fiber differed in length among studies due to anatomical restrictions related to the fiber implantation procedure (*i.e.*, size of the heart etc.). If we consider diffusive processes alone, the relative recovery (RR) can be expressed as:

$$RR = \frac{C_{inside}}{C_{outside}} = 1-\exp\left(-k\frac{A}{F}\right) = 1-\exp\left(-k\frac{mL}{F}\right)$$

where C_{inside} and $C_{outside}$ are the ACh concentrations inside and outside the dialysis fiber; A is the surface area of the dialysis membrane, which can be proportional to the fiber length L with a coefficient m; F is a perfusion flow rate; and k is the mass transfer coefficient (Ståhle 1991). The *in vitro* RR for ACh is approximately 70% with $F=2$ µl/min and $L=13$ mm (Akiyama et al. 1994), which yields $km=0.1852$. Using this value, the *in vitro* RR would be approximately 52% for $L=8$ mm and 31% for $L=4$ mm. Although these values provide some clues to speculate the effects of fiber length on the detected ACh concentrations, they cannot be directly extrapolated to the present results, because k should be different in *in vivo* conditions.

The physiological significance of vagal innervation of the left ventricle is controversial, because fixed-rate atrial pacing abolishes vagally induced inhibition of left ventricular contractility in an experimental setting without significant background sympathetic tone (Matsuura et al. 1997). On the other hand, when the cardiac sympathetic nerve is activated, vagal stimulation can reduce ventricular contractility even under fixed-rate atrial pacing by antagonizing the sympathetic effect (Nakayama et al. 2001). In addition, vagal stimulation suppresses myocardial interstitial myoglobin release during acute myocardial ischemia in anesthetized cats (Kawada et al. 2008). Chronic vagal stimulation improves the survival rate of rat models of chronic heart failure after myocardial infarction (Li et al. 2004). These lines of evidence suggest that vagal innervation of the left ventricle may be of therapeutic significance.

An unresolved question regarding the cardioprotective effects of vagal stimulation is that a large quantity of ACh is released in the ischemic region without vagal stimulation (Fig. 1). In the present

Table 3
Mean arterial pressure (AP) and heart rate (HR) obtained during Protocol 3 ($n=5$).

	Baseline	Vagal stimulation 20 Hz	Vagal stimulation 40 Hz	Recovery
AP (mm Hg)	100±3	59±9**	54±9**	86±5
HR (beats/min)	322±14	126±5**	100±8**	311±8

Data are shown as the mean±SE. $^{**}P<0.01$ vs. baseline based on Dunnett's test.

study, vagal stimulation at 20-Hz lowered the HR by approximately 200 beats/min (to less than 40% of the control value) but the stimulation-induced ACh release did not exceed the ischemia-induced ACh release (Figs. 1 and 3). On the other hand, vagal stimulation that reduced the HR by only 10% produces a significant increase in the survival rate of chronic heart failure rats (Li et al. 2004). Therefore, vagal stimulation probably exerts its beneficial effects not only within the ischemic region but also outside of this region. For instance, vagal stimulation in dogs with a healed myocardial infarction is known to prevent lethal arrhythmia induced by exercise (Vanoli et al. 1991). Afferent vagal activation may also contribute to the cardioprotective effects. Further studies are clearly needed to identify the mechanisms underlying the vagally induced cardioprotective effects against myocardial infarction and chronic heart failure.

Conclusion

The present study demonstrated the presence of vagal innervation in the rabbit left ventricle. Acute myocardial ischemia significantly increased the myocardial interstitial ACh levels. In addition, a brief ischemic event (5 min) caused detectable increases in ACh levels, indicating that endogenous ACh release may provide a trigger for ischemic preconditioning.

Acknowledgments

This study was supported by the Health and Labour Sciences Research Grants (H18-nano-Ippan-003, H19-nano-Ippan-009, H20-katsudo-Shitei-007, and H21-nano-Ippan-005) from the Ministry of Health, Labour and Welfare of Japan; by a Grant-in-Aid for Scientific Research (No. 20390462) from the Ministry of Education, Culture, Sports, Science and Technology of Japan; and by the Industrial Technology Research Grant Program from the New Energy and Industrial Technology Development Organization (NEDO) of Japan.

References

Akiyama T, Yamazaki T, Ninomiya I. In vivo detection of endogenous acetylcholine release in cat ventricles. American Journal of Physiology 266 (3 Pt 2), H854–H860, 1994.

Brown OM. Cat heart acetylcholine: Structural proof and distribution. American Journal of Physiology 231 (3), 781–785, 1976.

Cason BA, Gamperl AK, Slocum RE, Hickey RF. Anesthetic-induced preconditioning: Previous administration of isoflurane decreases myocardial infarct size in rabbits. Anesthesiology 87 (5), 1182–1190, 1997.

Cohen MV, Liu GS, Downey JM. Preconditioning causes improved wall motion as well as smaller infarcts after transient coronary occlusion in rabbits. Circulation 84 (1), 341–349, 1991.

Glantz SA. Primer of Biostatistics, 5th ed. McGraw-Hill, New York, 2002.

Kawada T, Yamazaki T, Akiyama T, Sato T, Shishido T, Inagaki M, Takaki H, Sugimachi M, Sunagawa K. Differential acetylcholine release mechanisms in the ischemic and non-ischemic myocardium. Journal of Molecular and Cellular Cardiology 32 (3), 405–414, 2000.

Kawada T, Yamazaki T, Akiyama T, Shishido T, Inagaki M, Uemura K, Miyamoto T, Sugimachi M, Takaki H, Sunagawa K. In vivo assessment of acetylcholine releasing function at cardiac vagal nerve terminals. American Journal of Physiology. Heart and Circulatory Physiology 281 (1), H139–H145, 2001.

Kawada T, Yamazaki T, Akiyama T, Mori H, Inagaki M, Shishido T, Takaki H, Sugimachi M, Sunagawa K. Effects of brief ischaemia on myocardial acetylcholine and noradrenaline levels in anaesthetized cats. Autonomic Neuroscience: Basic and Clinical 95 (1–2), 37–42, 2002.

Kawada T, Yamazaki T, Akiyama T, Li M, Ariumi H, Mori H, Sunagawa K, Sugimachi M. Vagal stimulation suppresses ischemia-induced myocardial interstitial norepinephrine release. Life Sciences 78 (8), 882–887, 2006a.

Kawada T, Yamazaki T, Akiyama T, Uemura K, Kamiya A, Shishido T, Mori H, Sugimachi M. Effects of Ca^{2+} channel antagonists on nerve stimulation-induced and ischemia-induced myocardial interstitial acetylcholine release in cats. American Journal of Physiology. Heart and Circulatory Physiology 291 (5), H2187–H2191, 2006b.

Kawada T, Yamazaki T, Akiyama T, Shishido T, Shimizu S, Mizuno M, Mori H, Sugimachi M. Regional difference in ischaemia-induced myocardial interstitial noradrenaline and acetylcholine releases. Autonomic Neuroscience: Basic and Clinical 137 (1–2), 44–50, 2007.

Kawada T, Yamazaki T, Akiyama T, Kitagawa H, Shimizu S, Mizuno M, Li M, Sugimachi M. Vagal stimulation suppresses ischemia-induced myocardial interstitial myoglobin release. Life Sciences 83 (13–14), 490–495, 2008.

Kilbinger H, Löffelholz K. The isolated perfused chicken heart as a tool for studying acetylcholine output in the absence of cholinesterase inhibition. Journal of Neural Transmission 38, 9–14, 1976.

Kitagawa H, Yamazaki T, Akiyama T, Sugimachi M, Sunagawa K, Mori H. Microdialysis separately monitors myocardial interstitial myoglobin during ischemia and reperfusion. American Journal of Physiology Heart and Circulatory Physiology 289 (2), H924–H930, 2005.

Krieg T, Qin Q, Philipp S, Alexeyev MF, Cohen MV, Downey JM. Acetylcholine and bradykinin trigger preconditioning in the heart through a pathway that induces Akt and NOS. American Journal of Physiology. Heart and Circulatory Physiology 287 (6), H2606–H2611, 2004.

Li M, Zheng C, Sato T, Kawada T, Sugimachi M, Sunagawa K. Vagal nerve stimulation markedly improves long-term survival after chronic heart failure in rats. Circulation 109 (1), 120–124, 2004.

Liu GS, Thornton J, Van Winkle DM, Stanley AW, Olsson RA, Downey JM. Protection against infarction afforded by preconditioning is mediated by A_1 adenosine receptors in rabbit heart. Circulation 84 (1), 350–356, 1991.

Matsuura W, Sugimachi M, Kawada T, Sato T, Shishido T, Miyano H, Nakahara T, Ikeda Y, Alexander Jr J, Sunagawa K. Vagal stimulation decreases left ventricular contractility mainly through negative chronotropic effect. American Journal of Physiology 273 (2 Pt 2), H534–H539, 1997.

Murry CE, Jennings RB, Reimer KA. Preconditioning with ischemia: A delay of lethal cell injury in ischemic myocardium. Circulation 74 (5), 1124–1136, 1986.

Nakayama Y, Miyano H, Shishido T, Inagaki M, Kawada T, Sugimachi M, Sunagawa K. Heart rate-independent vagal effect on end-systolic elastance of the canine left ventricle under various levels of sympathetic tone. Circulation 104 (19), 2277–2279, 2001.

Piper HM, Abdallah Y, Schäfer C. The first minutes of reperfusion: A window of opportunity for cardioprotection. Cardiovascular Research 61 (3), 365–371, 2004.

Przyklenk K, Kloner RA. Low-dose iv acetylcholine acts as a "preconditioning-mimetic" in the canine model. Journal of Cardiac Surgery 10 (4), 389–395, 1995.

Qin Q, Downey JM, Cohen MV. Acetylcholine but not adenosine triggers preconditioning through PI3-kinase and a tyrosine kinase. American Journal of Physiology. Heart and Circulatory Physiology 284 (2), H727–H734, 2003.

Richard V, Blanc T, Kaeffer N, Tron C, Thuillez C. Myocardial and coronary endothelial protective effects of acetylcholine after myocardial ischaemia and reperfusion in rats: Role of nitric oxide. British Journal of Pharmacology 115 (8), 1532–1538, 1995.

Shimizu S, Akiyama T, Kawada T, Shishido T, Yamazaki T, Kamiya A, Mizuno M, Sano S, Sugimachi M. In vivo direct monitoring of vagal acetylcholine release to the sinoatrial node. Autonomic Neuroscience: Basic and Clinical 148 (1–2), 44–49, 2009.

Snedecor GW, Cochran WG. Statistical Methods. Iowa State, Iowa, pp. 290–291, 1989.

Ståhle L. The use of microdialysis in pharmacokinetics and pharmacodynamics. In: Robinson, TE, JusticeJr. Jr, JB (Eds.), Microdialysis in the Neurosciences, pp. 155–174. Elsevier Science Ltd. New York, 1991.

Thames MD, Klopfenstein HS, Abboud FM, Mark AL, Walker JL. Preferential distribution of inhibitory cardiac receptors with vagal afferents to the inferoposterior wall of the left ventricle activated during coronary occlusion in the dog. Circulation Research 43 (4), 512–519, 1978.

Uemura K, Li M, Tsutsumi T, Yamazaki T, Kawada T, Kamiya A, Inagaki M, Sunagawa K, Sugimachi M. Efferent vagal nerve stimulation induces tissue inhibitor of metalloproteinase-1 in myocardial ischemia–reperfusion injury in rabbit. American Journal of Physiology. Heart and Circulatory Physiology 293 (4), H2254–H2261, 2007.

Vanoli E, de Ferrari GM, Stramba-Badiale M, Hull Jr SS, Foreman RD, Schwartz PJ. Vagal stimulation and prevention of sudden death in conscious dogs with a healed myocardial infarction. Circulation Research 68 (5), 1471–1481, 1991.

Yao Z, Gross GJ. Acetylcholine mimics ischemic preconditioning via a glibenclamide-sensitive mechanism in dogs. American Journal of Physiology 264 (6 Pt 2), H2221–H2225, 1993.

Effect of the cholinesterase inhibitor donepezil on cardiac remodeling and autonomic balance in rats with heart failure

Authors: Yoshihisa Okazaki [1,2], Can Zheng [2], Meihua Li [2], Masaru Sugimachi [1,2]

Institutions: [1] Department of Artificial Organ Medicine, Division of Surgical Medicine, Osaka University Graduate School of Medicine, Suita 565-0871, Japan

[2] Department of Cardiovascular Dynamics, Advanced Medical Engineering Center, National Cardiovascular Center Research Institute, Suita 565-8565, Japan

Correspondence: Masaru Sugimachi, MD, PhD

Department of Cardiovascular Dynamics, Advanced Medical Engineering Center, National Cardiovascular Center Research Institute, Suita 5658565, Japan

TEL: +81-6-6833-5012 x2509

FAX: +81-6-6835-5403

e-mail: su91mach@ri.ncvc.go.jp

Abstract

We have previously shown the beneficial effect of direct vagal electrical stimulation on cardiac remodeling and survival. In this study, we tried to reproduce the effect of vagal enhancement by administration of an acetylcholinesterase inhibitor, donepezil. A rat model of heart failure following extensive healed myocardial infarction was used. In rats given donepezil (5 mg/kg/day) in drinking water, biventricular weight was smaller (3.40±0.13 vs. 3.02±0.21 g/kg body weight, $p<0.05$), and maximal rate of rise (3256±955 vs. 3822±389 mmHg/s, $p<0.05$) and enddiastolic value (30.1±5.6 vs. 23.2±5.7 mmHg, $p<0.05$) of left ventricular pressure were improved. Neurohumoral factors were suppressed (norepinephrine, 1885±1423 vs. 316±248 pg/ml, $p<0.01$; BNP, 457±68 vs. 362±80 ng/ml, $p<0.05$). High frequency component of heart rate variability showed a nocturnal increase. These findings indicated that donepezil reproduced the anti-remodeling effect of electrical vagal stimulation. Further studies are warranted to evaluate the clinical usefulness of donepezil in heart failure.

(149 words)

Keywords

Myocardial infarction, Vagal stimulation, Heart rate variability, Neurohumoral activation

Introduction

Profound imbalance of the autonomic nervous system has been considered to be an important factor that aggravates heart failure [1]. The imbalance includes not only overactive sympathetic activity but also diminished vagal activity [2]. Various therapeutic agents including beta-blockers [3, 4], angiotensin converting enzyme inhibitors [5, 6], and angiotensin receptor antagonists [7, 8] have proven useful at least partly by correcting the abnormally augmented sympathetic activity. However, few endeavors have been made to actively remedy the reduced vagal activity as a treatment for heart failure. As the first attempt of this therapeutic strategy, our group has shown that in rats with aggravating chronic heart failure after experimentally-induced healed myocardial infarction, electrical stimulation of the vagus nerve markedly improved survival through prevention of cardiac remodeling [9].

Since the efferent vagal nerve activity is transmitted by acetylcholine, drugs that increase the acetylcholine concentration at the neuro-effector junction are expected to have the similar effect as electrical stimulation. In fact, clinical trials of the acetylcholinesterase inhibitor pyridostigmine have been conducted in patients with chronic heart failure [10, 11], resulting in decreased ventricular arrhythmia, enhanced heart rate variability at rest, increased heart rate reserve and oxygen pulse during exercise, as well as improved heart rate recovery after exercise. However, these studies examined the effect of short-term administration (one to two days), and the long-term effect of pyridostigmine has not been investigated. Clinical trials have also been conducted on scopolamine that stimulates vagus nerve centrally at low doses [12, 13]. Transdermal administration of a small dose of scopolamine in patients with heart failure following myocardial infarction increased heart rate variability and enhanced baroreflex sensitivity. These studies have not shown, however, anti-remodeling effect, more direct evidence against the progression of heart failure.

We hypothesized that donepezil, a novel acetylcholinesterase inhibitor, would show

various clinically-relevant beneficial effects through its preferential effects on neural true cholinesterase (rather than hepatic pseudocholinesterase) [14]. Therefore, in the present study, we investigated the effect of donepezil on hemodynamics, neurohumoral activation, and cardiac remodeling in rats with chronic heart failure. In addition, we analyzed high-frequency component of the heart rate variability to assess changes in vagal tone [15, 16]. The results indicated that donepezil reproduced anti-remodeling effect of electrical stimulation of the vagus nerve, and increased vagal tone.

Materials and Methods

The protocol of this study was performed in accordance with the Guiding Principles for the Care and Use of Animals in the Field of Physiological Sciences, and was approved by the Experimental Animal Committee of the National Cardiovascular Center.

Chronic heart failure model

Male Sprague-Dawley rats (8 weeks of age) were used. Under halothane anesthesia, a thoracotomy was performed and the main branch of the left coronary artery was ligated with nylon to produce myocardial infarction. The ligation resulted in myocardial infarction of 45 to 55%. The rats recovered from extensive myocardial infarction and progressed to the chronic state of heart failure (see Results). For ventricular fibrillation that occurred within one hour of ligation, defibrillation was conducted actively by cardiac massage in order to salvage as far as possible the rats with extensive myocardial infarction.

Experimental protocol

One week after induction of myocardial infarction, the surviving rats underwent another operation under halothane anesthesia. An electrocardiogram (ECG) telemetry device was implanted in each rat to monitor ECG and heart rate continuously (Figure 1A).

Rats that survived another week were divided into a nontreated group and a donepezil group. The donepezil group was administered the acetylcholinesterase inhibitor donepezil (Aricept®, Eisai, Tokyo, Japan) dissolved in drinking water at a concentration of 50 mg/dl. The dose estimated from the volume of water consumed was 5 mg/kg/day on average. The selection of donepezil rested on the fact that it more inhibits the (true) acetylcholinesterase at synapses and effectors but less inhibits pseudocholinesterase (butyrylcholinesterase) in liver than other drugs [14].

At week 6 after treatment was started (week 8 after infarction), 13 rats in the nontreated group and 14 rats in the donepezil group were subjected to hemodynamic study under halothane anesthesia. After hemodynamic study and blood collection, the rats were euthanized by overdose of halothane, and histological examination was conducted.

In other 11 rats with similar healed myocardial infarction, heart rate variability was calculated from the continuous ECG recordings between weeks 12 to 20 after myocardial infarction, In 11 rats, 5 served as the nontreated group (weeks 12-20 after infarction) and 6 received the donepezil treatment (weeks 17 to 19 after infarction). Preliminary analysis indicated no differences in heart rate variability at 8 weeks after infarction.

Hemodynamic measurement

At week 6 of the treatment period, hemodynamic study was conducted in rats under halothane anesthesia. A Millar catheter (SPC-320, Millar Instruments, Houston, TX) was inserted from the carotid artery into the left ventricle to measure left ventricular pressure with high fidelity. From the left ventricular pressures, the maximal first derivative of left ventricular pressure over time (dP/dt_{max}) and left ventricular enddiastolic pressure was calculated. The right atrial pressure was measured by an external transducer via a catheter filled with physiological saline.

Neurohumoral factor measurements

Three ml of blood was collected and the neurohumoral factors in blood were assayed. As indices of sympathetic activity, norepinephrine (NE) and epinephrine (Epi) were measured using by high-performance liquid chromatography with electrochemical detection. Plasma level of brain (or B-type) natriuretic peptide (BNP) was measured by ELISA assay (BNP-32 Enzyme Immunoassay Kit, Peninsula Lab, San Carlos, CA). We included BNP for its importance as a strong predictor of prognosis [17, 18]. BNP has been useful in detecting new patients with heart failure and in predicting the mortality and cardiac events in patients as well as in asymptomatic subjects. BNP may also be useful with heart failure with preserved systolic function.

Heart tissue examination

The left and right ventricles were excised and the total weight was measured. Next, both ventricles were sectioned into 3 mm-thick three slices, starting from the apex towards the base of the heart. Myocardial infarction size was assessed from the proportion of the length of infarct to the left ventricular perimeter measured on each section.

Power spectral analysis of heart rate variability

The ECG telemetric data were processed as follows. Signals from the transmitter model TA11CTA-F40 (Data Sciences International, St. Paul, MN) were recorded on a recording software HEM (Notocord, Newark, NJ). From the data of the continuous recording (1 kHz sampling), an analysis software HRT10a1 (Notocord, Newark, NJ) was used to extract the RR intervals. All the RR intervals were extracted from 24-hour continuous recording data for the nontreated and the donepezil groups. The text data of 2-hour intervals were stored in files to be analyzed later using the heart rate variability analysis software that we developed. Due to the frequent occurrence of extrasystoles in

chronic heart failure, it was necessary to develop an original algorithm to process the data as explained below.

Heart rate variability analysis software

The following procedures were conducted.

(1) Data preparation

The 2-hour data were combined to obtain 24-hour data. The time of R wave detection and the RR interval were saved as combined data.

(2) Removal of extrasystole

A 20-point median filter was applied to all the RR interval data to produce a sequence. Heart beats with RR intervals differing from the median value by 15 msec (threshold) or above were recognized and recorded as extrasystole or post-extrasystole. These data were excluded from analysis.

(3) Resampling of valid interval data

The 24-hour data were divided into 6-minute data (with 50% overlap). After excluding the RR intervals associated with extrasystole, the valid RR interval data were resampled at intervals of 1/10 seconds using linear interpolation.

(4) Power spectral analysis

In the power spectral analysis, 1024 points of 1/10-second data were grouped into a segment (segment length = 100.24 seconds) for fast Fournier transformation (FFT). The power spectra obtained from 6 segments were ensemble averaged. Prior to FFT, linear trend was removed from each segment

(5) Data selection

Even though extrasystoles are removed, segments with many deleted data cannot be expected to yield reliable power spectral analysis results. Therefore data with 40 or more extrasystoles within 6 minutes were excluded from analysis.

(6) Definition of high frequency component (HF)

In this study, the effect of bigeminy that occurs in heart failure was observed in the higher frequency range. Therefore we excluded frequency range > 1.5 Hz and HF was defined as the power from 0.5 to 1.5 Hz. Power of HF component was determined during daytime (6:00 to 18:00) and nighttime (18:00 to 6:00).

Statistical analysis

All data are presented as mean ± SD. Continuous variables were compared using unpaired t-test between two groups. The differences were considered significant when $p < 0.05$.

Results

Hemodynamics

Figure 2 shows the results of hemodynamic parameters measured under anesthesia 6 weeks after the onset of donepezil administration. A left ventricular pressure waveform and its first derivative are exemplified in Figure 2A. In this example (in a nontreated rat) the maximal first derivative of left ventricular pressure (dP/dt_{max}) was markedly decreased. In the donepezil group, dP/dt_{max} was significantly increased compared to the nontreated group (3822 ± 389 versus 3256 ± 955 mmHg/s, $p < 0.05$, Figure 2B). Left ventricular enddiastolic pressure (LVEDP; 23.2 ± 5.7 versus 30.1 ± 5.6 mmHg, $p < 0.05$, Figure 2C) and right atrial pressure (RAP; 4.1 ± 2.9 versus 7.0 ± 4.0 mmHg, $p < 0.05$, Figure 2D) was significantly lowered by donepezil administration. The contractility index dP/dt_{max} is known as a heart rate- and preload-dependent index. Because heart rate was higher in the nontreated group (354 ± 37 vs. 324 ± 23 bpm, difference ~9%) and LVEDP was higher in the nontreated group, the difference in heart rate and preload would have underestimated the true difference in contractility. Moreover, decreased LVEDP with decreased RAP in donepezil